Title

Tissue specific requirements for WNT11 in developing outflow tract and dorsal mesenchymal protrusion

Journal

Developmental Biology, 429(1)

ISSN

0012-1606

Authors

van Vliet, Patrick P
Lin, Lizhu
Boogerd, Cornelis J
et al.

Publication Date

2017-09-01

DOI

10.1016/j.ydbio.2017.06.021

Peer reviewed

HHS Public Access

Author manuscript

Dev Biol. Author manuscript; available in PMC 2017 September 01.

Published in final edited form as:

Dev Biol. 2017 September 01; 429(1): 249–259. doi:10.1016/j.ydbio.2017.06.021.

Tissue specific requirements for WNT11 in developing outflow tract and dorsal mesenchymal protrusion

Patrick P. van Vliet[a,2,1], **Lizhu Lin**[a,b,1], **Cornelis J. Boogerd**[a], **James F. Martin**[c], **Gregor Andelfinger**[d], **Paul D. Grossfeld**[b,*], and **Sylvia M. Evans**[a,e,f,**]

[a]Skaggs School of Pharmacy and Pharmaceutical Sciences, UCSD, La Jolla, USA

[b]Department of Pediatrics, School of Medicine, UCSD, La Jolla, USA

[c]Baylor College of Medicine, Texas Heart Institute, Houston, USA

[d]Department of Pediatrics, CHU Sainte Justine, Montréal, Canada

[e]Department of Medicine, UCSD, La Jolla, USA

[f]Department of Pharmacology, UCSD, La Jolla, USA

Abstract

Correct cardiac development is essential for fetal and adult life. Disruptions in a variety of signaling pathways result in congenital heart defects, including outflow and inflow tract defects. We previously found that WNT11 regulates outflow tract development. However, tissue specific requirements for WNT11 in this process remain unknown and whether WNT11 is required for inflow tract development has not been addressed. Here we find that germline *Wnt11* null mice also show hypoplasia of the dorsal mesenchymal protrusion (DMP), which is required for atrioventricular septation. Ablation of *Wnt11* with myocardial *cTnTCre* recapitulated outflow tract defects observed in germline *Wnt11* null mice, but DMP development was unaffected. In contrast, ablation of *Wnt11* with *Isl1Cre* fully recapitulated both outflow tract and DMP defects of *Wnt11* germline nulls. DMP hypoplasia in *Wnt11* mutants was associated with reduced proliferation within the DMP, but no evident defects in myocardial differentiation of the DMP. Examination of *Pitx2*-, *Axin2*-, or *Patched-lacZ* reporter mice revealed no alterations in reporter expression, suggesting that WNT11 was required downstream of, or in parallel to, these signaling pathways to regulate DMP formation. These studies revealed a previously unappreciated role for WNT11 for DMP formation and distinct tissue-specific requirements for WNT11 in outflow tract and DMP development.

[*]Correspondence to: UC San Diego, Department of Pediatrics, Division of Pediatric Cardiology, 3020 Children's Way MC 5004, San Diego, CA 92123, USA. [**]Correspondence to: UC San Diego, Skaggs School of Pharmacy, 9500 Gilman Drive MC0613C, La Jolla, CA 92093, USA.

[1]Equal contribution.

[2]Present address: CHU Sainte Justine Research Center, Montréal, Canada.

Author contributions

PPV and SME designed experiments and wrote the manuscript. PPV performed experiments. LL made the *Wnt11* floxed mouse line and helped with maintenance of mouse lines. CJB helped setting up the cell quantification. JFM provided the *Pitx2-lacZ* mouse line. PPV, LL, CJB, GA, PDG, and SME analyzed data and revised the manuscript.

Keywords

Wnt11; Heart; Outflow tract; Dorsal mesenchymal protrusion

1. Introduction

Proper heart formation and separation of systemic and pulmonary circulation is vital for distribution of oxygen and nutrients. Myocardial cells of the heart derive from two heart fields defined by their temporal and spatial contribution to heart development (Buckingham et al., 2005; Evans et al., 2010). The first heart field contributes to most myocytes within the left ventricle as well as some atrial cells, while the second heart field contributes to a majority of myocytes within outflow tract (OFT), right ventricle, atria, and inflow tract (IFT). The second heart field can be further divided into an anterior second heart field (aSHF) that contributes to the developing OFT and right ventricle, and a posterior second heart field (pSHF) that contributes cells to the atria and IFT (Galli et al., 2008). Subsequent septation of the aorta and pulmonary artery is additionally dependent on mesenchymal cells from the cardiac neural crest and endocardium-derived outflow cushions (Anderson et al., 2016; Evans et al., 2010; Lin et al., 2012). Atrioventricular septation into left and right components is a highly complex event requiring input from second heart field-derived atrial myocardium, the endocardium-derived mesenchymal cap (MC) of the primary atrial septum, endocardium-derived atrioventricular cushions (AVC), and the dorsal mesenchymal protrusion (DMP) (Briggs et al., 2012; Burns et al., 2016; Kim et al., 2001; Lin et al., 2012). The DMP is a pSHF-derived mesenchymal tissue that starts to protrude from the dorsal mesocardium into the atrial lumen around embryonic day 10 (E10) in the mouse (Anderson et al., 2014; Mommersteeg et al., 2006). Incomplete or aberrant septation results in OFT defects and/or atrioventricular septal defects (AVSDs), which contribute to 3.7% (OFT) and 4.7% (AVSD) of all birth defects in humans (Parker et al., 2010). A better understanding of signaling pathways regulating cardiac septation is essential to improve diagnostics and treatment of patients.

Development of OFT and IFT is regulated by several overlapping signaling pathways, including WNT11 signaling (for a comprehensive overview, see Lin et al. (2012)). WNTs are secreted signaling molecules with subfamilies traditionally being divided into canonical and non-canonical pathways. Canonical WNT signaling acts via stabilization of beta-CATENIN, which is involved in both cell-cell adhesion and transcriptional activation of downstream targets. The beta-CATENIN-independent non-canonical WNT pathways act via cell polarity pathways and calcium signaling to determine cell function, adhesion, migration, and differentiation (Flaherty and Dawn, 2008).

We previously showed that non-canonical WNT11 is highly expressed in developing murine OFT where it directs proper OFT formation by regulating cell migration and differentiation via non-canonical WNT signaling (Zhou et al., 2007). Germline *Wnt11* null mice die embryonically and perinatally from OFT defects including double outlet right ventricle (DORV) and transposition of the great arteries (TGA). OFTs of *Wnt11* null mice demonstrate no differences in proliferation or apoptosis, but demonstrate perturbed

cytoskeletal and apical-basal arrangements, as observed in other mutants affecting non-canonical WNT signaling (Henderson et al., 2006).

Despite the well-described role of WNT11 in OFT development, it remains unclear if WNT11 is required for IFT development. A recent report showed high Wnt11 mRNA expression in the posterior dorsal mesocardium at embryonic day 10.5 (E10.5) (Cohen et al., 2012), suggesting a potential role in IFT development, in addition to its known role in OFT development. Labeling of *Wnt11* lineages with a tamoxifen-inducible *Wnt11CreERT2* showed contribution of *Wnt11*-lineage traced cells, when labeled at E8.0 or later, to both OFT endocardium and myocardium from E9.5 onwards (Sinha et al., 2015). *Wnt11* lineages, labeled between E7.0–9.0, contribute to IFT endocardium, but not myocardium, when examined between E9.0–10.5 (Sinha et al., 2015). Thus, WNT11 is spatiotemporally expressed in multiple cell lineages that are required for distinct aspects of heart development. The aims of the current study were to examine a potential role for WNT11 in IFT formation, and to further identify tissue specific requirements for WNT11. Our results showed that, indeed, WNT11 plays a broader role in cardiac development than previously appreciated, and that WNT11 is required in *cTnTCre* myocardial lineages for OFT development and within *Isl1Cre* lineages for normal development of the DMP.

2. Materials and methods

2.1. Mice

Germline *Wnt11* null (Majumdar et al., 2003), *Isl1Cre* (Yang et al., 2006), *cTnTCre* (Jiao et al., 2003), *Rosa26 flox-stop-flox tdTomato* (Rosa tdTom, line Ai14, B6;129S6 mixed background) (Madisen et al., 2010), *Pitx2-lacZ* (Kitamura et al., 1999), *Patched-lacZ* (Goodrich et al., 1997), and *Axin2-lacZ* (Lustig et al., 2002) mouse lines were previously described. Mice were maintained on a 129S4/SvJaeJ background (Jackson Laboratory #009104) and genotyping was performed as described. Animal care and experimental procedures were performed according to the NIH Guide for the Care and Use of Laboratory Animals as well as institutional guidelines and approved by the Institutional Animal Care and Use Committee at UC San Diego. Noon of the day of the vaginal plug was designated E0.5. Developmental stages were confirmed by somite counting (up to E11.5) and/or global morphology.

2.2. Generation of the Wnt11 floxed mouse line

The genomic sequence for *Mus musculus* wingless-type MMTV integration site family member 11 (*Wnt11*, NC_000073.6) is located on chromosome 7 and spans ten exons encoding six mRNA splice variants. Variants 1–5 all contain exon 3 (the first coding exon) and exon 4 (containing lipidation/palmitoylation and glycosylation sites required for adequate protein folding and transport). Only variants 1, 2, and 5 are protein-coding variants, whereas variants 3, 4, and 6 are non-protein coding and/or undergo nonsense mediated decay (GRCm38/mm10, http://www.ensembl.org). For the original *Wnt11* null allele (Majumdar et al., 2003), exons 4 and 5 were deleted, resulting in a stable, but nonfunctional transcript containing the signal peptide sequence and an out of frame sequence downstream of exon 3. However, deletion of exon 4 alone results in a frame shift between exon 3 and exon 5 and a

transcript that contains three novel stop-gain codons in exon 5, effectively eliminating production of a functional WNT11 protein. Exon 4 was therefore targeted to generate a floxed *Wnt11* allele.

The targeting construct for the floxed *Wnt11* allele contained a copy of the *Wnt11* genomic sequence (mouse genome version GRCm38/mm10) with 5′ and 3′ 4 kb homology arms (Fig. 2A). LoxP sites were placed 5′ and 3′ of exon 4 and a Frt-flanked Mcl-neomycin selection cassette was placed between the 3′ loxP site and exon 5. The targeting construct was transfected into 129S4/SvJ mouse embryonic stem cells and recombined clones selected with G418. Southern blot analysis was performed with a probe 3′ of exon 6 to screen ES cell genomic DNA after digestion with *Nde*I (Fig. 2B). Correctly targeted clones were microinjected in C57Bl/6 mouse blastocysts and F1 offspring were genotyped by PCR for the presence of the flox-neo insertion (Fig. 2C and data not shown). The Frt-flanked neomycin cassette was removed by crossing *Wnt11 flox-neo/+* mice to Flpase mice (Jax stock #012930), resulting in neomycin-negative *Wnt11 flox/+* offspring. *Wnt11 flox/+* mice were crossed with *Rosa-tdTomato* reporter mice to generate double heterozygous *Wnt11 flox/+; Rosa-tdTom/+* off-spring. Double heterozygous mice from different sublines were back-crossed twice to 129S4/SvJaeJ mice and offspring were intercrossed to generate double homozygous *Wnt11 flox/flox; Rosa-tdTom/tdTom* mice. Double homozygous mice are healthy and viable and do not show any abnormalities. Double homozygous *Wnt11 flox/flox; tdTom/tdTom* females were crossed with double heterozygous *Cre+/Wnt11-null* males to delete *Wnt11* in specific cells/tissues and simultaneously analyze the *Cre*-lineage. Primer sequences for the non-recombined *Wnt11* flox/flox allele are Forward: 5′-GAG TGT CCT TGC GTT ATT GAA T-3′ and Reverse: 5′-ATC TGT AAG GCA CTT CCA GCT G-3′. Primer sequences for the recombined Wnt11 flox/flox allele are Forward: 5′-GAG TGT CCT TGC GTT ATT GAA T-3′ and Reverse: 5′-GTG TGC TCT CCA GCA GTC TCA T-3′. The Wnt11 < flox > mouse line will be available from the Jackson Laboratory as JAX#030051.

2.3. Histology

Embryos were isolated from timed-pregnant females, dissected in ice-cold PBS, and fixed in ice-cold 4% paraformaldehyde (EMS 15710) in PBS. A minimum of four embryos were analyzed for each stage. Embryos were dehydrated, embedded, and sectioned as previously described (Boogerd et al., 2016). For hematoxylin and eosin staining, paraffin-embedded sections were rehydrated and stained with Gill's #1 hematoxylin (Sigma GHS132), washed, incubated in Bluing Reagent (Thermo Scientific 6769001), washed, stained in alcoholic eosin Y (Sigma HT110132), dehydrated, and embedded in Permount (Fisher SP15-100). Stained slides were imaged on a Hamamatsu Nanozoomer and processed with NDP View 2 software.

2.4. X-gal staining

Embryos were isolated in ice-cold PBS, fixed in 0.125% glutaraldehyde, 2% paraformaldehyde in PBS for 5–10 min on ice, and washed in ice-cold PBS. Whole mount embryos were stained according to the 'Bacterial beta-Galactosidase Histochemistry Bible' as described by Dr. Eric Mercer (http://wmc.rodentia.com/docs/lacZ_bible.html) (Mercer et

al., 1991). Embryos were washed three times for one hour each in 'rinsing buffer′ (PBS pH 7.5, 2 mM $MgCl_2$, 0.01% sodium deoxycholate, and 0.02% NP-40) at 4 °C and stained overnight at 37 °C in pre-warmed staining buffer (rinse buffer + 5 mM potassium ferricyanide, 5 mM potassium ferrocyanide, and 1 mg/ml X-gal from Thermo Fisher 15520-018). The next day, stained embryos were post-stained in rinse buffer for 15 min at 37 °C, washed three times in PBS at 4 °C, and fixed overnight in 4% paraformaldehyde in PBS at 4 °C. Stained embryos were imaged and dehydrated for paraffin embedding as described (Boogerd et al., 2016), except that xylene steps were kept to a maximum of 5 min. Paraffin-embedded embryos were sectioned at 10 μm, rehydrated, counterstained with Nuclear Fast Red (Sigma N3020), dehydrated, embedded in Permount, and imaged on a Hamamatsu Nanozoomer.

2.5. Immunofluorescence staining

EdU injection and staining was performed with the Click-iT EdU imaging kit (Molecular Probes C10340) as described (Boogerd et al., 2016). For immunofluorescence staining, cryosections were permeabilized in 0.5% Triton X-100 in PBS and blocked in blocking buffer (10% donkey serum, 1% BSA, 0.1% Triton X-100 in PBS) at RT for one hour, incubated with primary (o/n) or secondary antibodies and DAPI (2 h) in blocking buffer at 4 °C, washed, and mounted with DAKO mounting medium (VWR S3023). Stained slides were imaged on an Olympus FV1000 confocal or Leica DMi8 microscope. Antibodies used for immunostaining were ISL1 (Abcam ab109517, 1:100), NKX2-5 (Santa Cruz sc8697X, 1:400), PECAM/CD31 (BD Biosciences 550274, 1:50), ACTN2 (A7811; 1:200; Sigma-Aldrich), cleaved CASPASE-3 (9664; 1:200; Cell Signaling Technology), mouse Fab fragments (Jackson 715-007-003, 1:100), and AlexaFluor-conjugated secondary antibodies (Invitrogen).

2.6. Cell quantification

Cell counting experiments were performed as described previously in every third section of three biological replicates (Boogerd et al., 2016). Quantification of labeled and total cell numbers was performed by automatic counting in a region of interest with Perkin Elmer Volocity software. Relative numbers were calculated by comparing labeled cells to the total number of DAPI+ nuclei. Statistical differences were calculated with two-tailed, unpaired T-tests.

3. Results

3.1. Germline Wnt11 null mice develop IFT as well as OFT defects

Previous whole mount analysis of germline *Wnt11* null mice revealed abnormal OFT development from E9.5 onwards, resulting from defective cell polarity (Zhou et al., 2007). Detailed histological analysis confirmed that OFTs of *Wnt11* null mice appeared straighter, lacking the normal OFT rotation apparent in wild-type controls (Fig. 1A). These early malformations in *Wnt11* null mice led to DORV (Fig. 1B–C) or TGA (Zhou et al., 2007) at E11.5 and E14.5, as described previously. In accordance with earlier reports, we also observed ventricular septal defects (VSDs) and minor thinning of the ventricular myocardial wall (Fig. 1C) (Nagy et al., 2010; Zhou et al., 2007).

Posteriorly, atrioventricular septation requires a coordinated organization of the primary atrial septum (PAS), atrioventricular cushion (AVC), and dorsal mesenchymal protrusion (DMP) (Briggs et al., 2012; Burns et al., 2016). Starting around E9.5-E10.0, the SHF-derived DMP expands on the right side of the pulmonary ridges and protrudes into the atrial lumen in wild-type mouse embryos (Fig. 1A) (Anderson et al., 2014). Around E11.5, the DMP has connected dorsally with the endocardium-derived mesenchymal cap (MC) on the PAS and ventrally with the AVC, closing the posterior connection between left and right atria (Fig. 1B). After E11.5, the MC and DMP lose their mesenchymal phenotype and begin to myocardialize, resulting in a fully developed atrioventricular septum around E14.5 (Fig. 1C).

Histological comparison of *Wnt11* null embryos revealed no notable differences in PAS or AVC morphology when compared to wild-type controls (Fig. 1A and Supplementary Fig. 1). At E9.5, formation of the dorsal mesocardium appeared comparable in *Wnt11* null embryos and controls (Supplementary Fig. 1). In contrast, at E10.5, *Wnt11* null mutants demonstrated impaired development of the DMP, with mutants displaying a smaller right-sided DMP (Fig. 1A), and, at E11.5, exhibited a failure to close the connection between the MC and AVC (Fig. 1B). At E14.5, although the atrioventricular septum in *Wnt11* null mice had closed, the DMP remained significantly reduced in size (Fig. 1C).

3.2. Myocardial ablation of Wnt11 results in OFT defects but normal DMP formation

To examine tissue specific requirements for WNT11, we generated a *Wnt11* conditional mutant mouse line in which *Wnt11* could be deleted via Cre-LoxP mediated recombination (Fig. 2A–C and Section 2). The occurrence of OFT defects in *Wnt11* null embryos and high expression of WNT11 in OFT myocardium (Zhou et al., 2007) suggested a specific requirement for WNT11 in myocardium. We therefore ablated *Wnt11* in myocardial lineages with *cTnTCre* (Jiao et al., 2003). At E14.5, whole mount *cTnTCre; Wnt11* conditional knock-out (cKO) embryos appeared grossly phenotypically normal when compared to wild-type controls (Fig. 2D). However, histological analysis revealed that E14.5 *cTnTCre; Wnt11* cKO embryos exhibited TGA (Fig. 2E), consistent with a requirement for WNT11 in the myocardial lineage for OFT formation. In contrast to germline *Wnt11* null mice, *cTnTCre; Wnt11* cKO embryos did not show DMP abnormalities (Fig. 2E).

3.3. Ablation of Wnt11 with Isl1Cre recapitulates the cardiac phenotype of germline Wnt11 knockouts

Both OFT and IFT structures derive from the SHF, which is marked by ISL1 expression (Evans et al., 2010). To test whether ablation of *Wnt11* in *Isl1Cre* lineages could recapitulate the germline *Wnt11* null cardiac phenotype, we deleted *Wnt11* utilizing *Isl1Cre* (Yang et al., 2006). *Isl1Cre; Wnt11* cKO whole mount embryos were grossly normal at E12.5 and E14.5 when compared to wild-type controls (Fig. 3A–B). Histological analysis showed that E12.5 and E14.5 *Isl1Cre; Wnt11* cKO embryos exhibited DORV and TGA, respectively, similar to germline *Wnt11* null mice (Fig. 3C–D). Similar to germline *Wnt11* null mice, the connection between MC and AVC failed to fully develop in E12.5 *Isl1Cre; Wnt11* cKO embryos, suggesting reduced or delayed contribution of the DMP to AV septal closure (Fig. 3C). Further analysis at E14.5 revealed a smaller DMP-derived myocardial structure in

Isl1Cre; Wnt11 cKO embryos, comparable to the DMP defects observed in germline *Wnt11* null mice (Fig. 3D).

Isl1Cre marks a number of lineages that contribute to heart formation, including myocardial progenitors of the second heart field that directly contribute to the DMP, as well as endocardial, neural crest, and epicardial lineages (Cai et al., 2003; Engleka et al., 2012; Ma et al., 2008). In addition to myocardium, WNT11 is expressed in a variety of cell lineages required for heart development, including epicardium and endocardium (Cohen et al., 2012; Sinha et al., 2015; Zhou et al., 2007). To further investigate subsets of cell lineages marked by *Isl1Cre* in which WNT11 might be required for DMP formation, we ablated *Wnt11* in epicardial cells with *Wt1Cre* (Del Monte et al., 2011; Wessels et al., 2012) and in endocardial cells with *Tie2Cre* (Kisanuki et al., 2001). O'spring from these crosses were morphologically indistinguishable from wild-type controls and histological analysis revealed no OFT or DMP defects (data not shown). We also investigated a potential contribution of WNT11 in neural crest lineages to OFT formation, utilizing *Wnt1Cre2* (Lewis et al., 2013), but found no defects in either OFT or IFT (data not shown). Together, these results suggested that WNT11 was required for OFT and DMP formation in a subset of *Isl1Cre* lineages that did not include neural crest, epicardial, or endocardial lineages.

3.4. Wnt11 null mutant DMPs exhibit reduced proliferation but no alterations in apoptosis

Between E9.5 and E10.5, proliferation of ISL1-expressing pSHF cells results in expansion and protrusion of the developing DMP (Anderson et al., 2014; Briggs et al., 2013; Snarr et al., 2007a), whereas a reduction in ISL1 expressing DMP precursor cells is correlated with DMP hypoplasia (Bax et al., 2010; Briggs et al., 2013; Tian et al., 2010). Immunofluorescence staining and quantification at E10.5 confirmed DMP hypoplasia in germline *Wnt11* null mutants when quantified as total DAPI+ or ISL1+ nuclei (Fig. 4A–B), consistent with our earlier histological analysis (Fig. 1). In contrast, there was no difference in absolute number of cells in the pSHF (Fig. 4C), which we defined as the ISL1+ region between lung bud mesenchyme and dorsal border of the NKX2-5+ atrial wall (Fig. 4A) (Snarr et al., 2007a). To investigate whether proliferation defects could explain the reduced size of the DMP in KO embryos, we performed EdU labeling, and counted EdU+ cells in the protruding DMP as well as in the pSHF at E10.5 (Fig. 4A). Quantification of EdU+ cells revealed that, within the DMP, the frequency of proliferating cells was significantly reduced in *Wnt11* null mutants when compared to that of wild-type mice (Fig. 4D). In contrast, the frequency of proliferating cells in the pSHF was comparable between *Wnt11* mutants and controls (Fig. 4E). No differences in frequency of cleaved-CASPASE 3+ apoptotic cells were observed in either DMP or pSHF when comparing *Wnt11* mutants to controls (Fig. 4D–E). Together, these observations suggested that reduced proliferation within the DMP itself contributed to the DMP hypoplasia observed in *Wnt11* null mutants.

3.5. Myocardial differentiation of DMP is not altered in Wnt11 mutants

Upon closure of the gap between MC and AVC around E11.5, mesenchymal cells of the DMP begin to undergo myocardial differentiation, or "myocardialize" (Anderson et al., 2014; Snarr et al., 2007a). WNT11 is required for normal protrusive behavior of myocardial cells into the OFT cushions during OFT remodeling (Zhou et al., 2007) and can stimulate

cardiomyogenic differentiation (Flaherty and Dawn, 2008). Moreover, premature myocardial differentiation of the pSHF contributes to DMP defects (Bax et al., 2010; Goddeeris et al., 2008). Expression of NKX2-5 is an indicator of myocardial differentiation of the DMP (Snarr et al., 2007a). Therefore, to assess whether the pSHF or DMP in *Wnt11* germline null mutants had undergone premature differentiation, we quantified the number of NKX2-5+ cells in the pSHF and protruding DMP at E10.5 (Fig. 4A). However, we did not observe a difference in the absolute or relative number of NKX2-5+ cells in either protruding DMP or pSHF (Fig. 4D–E).

Since most myocardial differentiation of the DMP occurs after E11.5 (Snarr et al., 2007a, 2007b), we additionally examined the *Isl1Cre*-lineage in E12.5 *Isl1Cre; Wnt11* cKO mutants by staining for alpha-sarcomeric actin (SAA), which strongly labels the sarcomeric structures of cardiomyocytes. As expected, SAA labeling was evident in the myocardium of the atrial wall, atrial septum, and the DMP-derived myocardium between atrial septum and AVC in control embryos (Fig. 4F). The reduced numbers of DMP cells in *Isl1Cre; Wnt11* cKOs appeared to have differentiated normally, as evidenced by SAA expression (Fig. 4F). Together, these results suggested that DMP defects in *Wn11* germline null and *Isl1Cre; Wnt11* cKO mutants did not arise from premature or aberrant myocardial differentiation.

3.6. No alterations in PITX2, SHH, or canonical WNT signaling in Wnt11 null mouse hearts

To gain further understanding of proliferative defects within the DMP observed in *Wnt11* mutants, we examined several signaling pathways that regulate proliferation and are required for normal DMP development. The bicoid related homeodomain transcription factor paired-like homeodomain 2, PITX2, is expressed in left-sided structures of the heart and lungs and regulates growth and morphogenesis of SHF-derived lineages in OFT, atrioventricular region, and IFT (Ai et al., 2006; Kitamura et al., 1999; Mommersteeg et al., 2007). To examine whether PITX2 expression was affected in *Wnt11* germline null mutants, we analyzed expression of *Pitx2-lacZ*, which expresses lacZ under the influence of the endogenous *Pitx2* locus (Kitamura et al., 1999). Consistent with our earlier findings, E10.5 *Wnt11* null mutants showed OFT and DMP defects at E10.5 (Fig. S1). However, *Pitx2-lacZ* expression in *Wnt11* mutants did not appear altered in either OFT, dorsal atrial wall, or left of the DMP when compared to controls (Fig. 5A), suggesting that loss of WNT11 did not affect PITX2 expression.

OFT and atrial septation rely heavily on the sonic hedgehog (SHH) signaling pathway (Briggs et al., 2016; Goddeeris et al., 2008, 2007; Hoffmann et al., 2009; Lin et al., 2006; Washington Smoak et al., 2005). SHH, which is expressed and secreted in pharyngeal and pulmonary endoderm, activates expression of Patched homolog-1 (PTCH1) in SHH-receiving cells of the anterior and posterior SHF, including those that give rise to the DMP, between E8.5–10.5 (Goddeeris et al., 2007; Hoffmann et al., 2009; Washington Smoak et al., 2005). To assess whether OFT or DMP defects in *Wnt11* germline null mutants could be explained by altered SHH signaling, we analyzed expression of *Ptch1-lacZ* as an indicator of hedgehog signaling (Goodrich et al., 1997). Although E10.5 *Wnt11* germline null mutants showed OFT defects and a smaller DMP, *Ptch1-lacZ* expression was not significantly altered in OFT, dorsal atrial wall, or the remaining DMP when compared to controls (Fig. 5B). This

suggested that defects observed in *Wnt11* germline null mutants did not arise from altered SHH signaling.

Development of SHF-derived structures depend on beta-CATENIN-dependent canonical WNT signaling, which acts upstream of non-canonical WNT signaling by WNT11 (Ai et al., 2007; Bosada et al., 2016; Briggs et al., 2016; Lin et al., 2007; Qyang et al., 2007; Tian et al., 2010). Non-canonical WNT signaling can reciprocally repress canonical WNT signaling (Abdul-Ghani et al., 2011; Bisson et al., 2015; Cohen et al., 2012). To test whether canonical WNT signaling was increased or altered consequent to loss of WNT11 in *Wnt11* germline null mice, we analyzed expression of *Axin2-lacZ*, which accurately reflects activation of canonical WNT signaling in proximal OFT and AVC myocardium and mesenchyme (Bosada et al., 2016; Gillers et al., 2015; Lustig et al., 2002). As expected, *Wnt11* germline null embryos exhibited OFT and DMP defects. However, *Axin2-lacZ* expression in OFT, AVC, or the SHF was not altered when compared to controls (Fig. 5C), suggesting that, in *Wnt11* mutants, canonical WNT signaling was not altered.

Together these observations indicated that no significant alterations in PITX2 expression or signaling by the hedgehog or canonical WNT pathways had occurred within the heart consequent to loss of WNT11. These data suggested that WNT11 may act downstream of, or in a pathway parallel to these pathways to effect DMP formation.

4. Discussion

WNT signaling regulates various aspects of early and late embryogenesis and is essential for proper development of the heart. Non-canonical WNT signaling by the secreted ligand WNT11 is known to affect cell proliferation, differentiation, and polarized cell migration (Flaherty and Dawn, 2008; Uysal-Onganer and Kypta, 2012). We and others showed previously that WNT11 regulates myocardialization of the outflow tract and that loss of WNT11 results in altered cell polarity and, consequently, OFT defects (Nagy et al., 2010; Zhou et al., 2007). Here, we showed that WNT11 was also required for DMP formation in germline *Wnt11* null mice by regulating DMP proliferation and dissected cell-specific requirements for WNT11 for both OFT and DMP formation by conditional ablation of *Wnt11* in multiple cell types required for heart formation.

WNT11 is initially expressed in the endocardium and the myocardium of the embryonic common atrium, ventricle, and OFT at E8.5, and in the myocardium of the outflow tract and atria, the anterior and posterior SHF, endocardium, epicardium, and the ventral mesenchyme of the lung buds at E10.5 (data not shown) (Cohen et al., 2012; Sinha et al., 2015). To investigate tissue specific requirements for WNT11 in OFT and IFT, we generated a *Wnt11 flox/flox* mouse line. No cardiac phenotypes were observed when *Wnt11* was ablated with *Tie2Cre* (Kisanuki et al., 2001), *Wt1Cre* (Del Monte et al., 2011; Wessels et al., 2012), or *Wnt1Cre2* (Lewis et al., 2013) (data not shown). This suggested that WNT11 expression in endothelial, endocardial, epicardial, or cardiac neural crest was not required for cardiac morphogenesis, despite high expression of WNT11 in particular in endocardial and epicardial cells (Sinha et al., 2015).

The germline *Wnt11* null OFT phenotype was recapitulated by ablation of *Wnt11* in *cTnTCre* myocardial- and *Isl1Cre* SHF-derived lineages (Figs. 2 and 3). As *Isl1Cre* lineages give rise to myocardium of the OFT, these data suggest that the previously analyzed OFT phenotype of *Wnt11* germline nulls, i.e. aberrant polarization and protrusion of myocytes and subsequent defective myocardialization within the OFT (Zhou et al., 2007), reflects a myocardial intrinsic requirement for WNT11 for these behaviors.

Both *Wnt11* germline nulls and *Isl1Cre; Wnt11* cKO mutants showed both OFT and DMP phenotypes, the latter evidenced as smaller DMPs and a consequently reduced contribution to atrial septation. The OFT and DMP defects are likely to occur independently, since *cTnTCre; Wnt11* cKO embryos showed OFT defects, but no DMP defects.

The DMP derives from the ISL1 expressing SHF and differentiates following protrusion into the atrial lumen and connection to the mesenchymal cap and the superior and inferior atrioventricular cushions (Anderson et al., 2014). We found that WNT11 was required in *Isl1Cre* lineages (Fig. 3), but not *cTnTCre* lineages (Fig. 2), for DMP development. These results indicated that WNT11 was required prior to myocardial differentiation in ISL1 expressing populations for DMP formation. Potentially relevant ISL1 expressing populations include both SHF progenitors and foregut endoderm. WNT11 is expressed in foregut endoderm between E6 and E7 (Sinha et al., 2015). In contrast, ISL1 is first expressed in foregut endoderm at E7.5 (Cai et al., 2003; Prall et al., 2007). Therefore, ablation with *Isl1Cre* would be too late to affect WNT11 expression in pharyngeal endoderm. Altogether, the foregoing observations indicate that WNT11 is required within Isl1Cre expressing SHF progenitors prior to their differentiation for DMP formation.

Reduced proliferation, increased apoptosis, and/or reduced or premature myocardial differentiation can lead to defective DMP development and, consequently, AVSD (Briggs et al., 2012). Upon germline deletion of *Wnt11*, we observed reduced proliferation in the DMP itself but not in the SHF dorsal to the DMP (Fig. 4). We found no differences in apoptotic cells in either DMP or SHF, suggesting that ablation of *Wnt11* does not differentially affect cell survival during the stages analyzed. No reduced or premature myocardial differentiation of the DMP was observed.

To further investigate the mechanisms by which WNT11 might be required to drive proliferation of DMP, we examined potential interactions between WNT11 and several other pathways previously shown to be required for proliferation of the DMP, including sonic hedgehog, canonical WNT, and PITX2 pathways (Burns et al., 2016). Ablation of the POU-homeodomain transcription factor *Pitx2* leads to OFT and atrial septation defects (Kitamura et al., 1999). Given the role of PITX2 in atrial septation, we wondered whether there might be any effect of *Wnt11* ablation on PITX2 expression during DMP formation. However, examination of *Pitx2-lacZ* in *Wnt11* null mutants did not reveal perturbation of PITX2 expression (Fig. 5A). As we previously found that PITX2 was upstream of WNT11 for OFT formation (Zhou et al., 2007), it would be of future interest to examine whether PITX2 may also be upstream of WNT11 in DMP formation.

Previous studies have demonstrated that signaling from the hedgehog receptor smoothened (SMO) is required within SHF lineages to drive proliferation of DMP precursors in the SHF (Briggs et al., 2016; Goddeeris et al., 2008, 2007; Hoffmann et al., 2009; Lin et al., 2006; Washington Smoak et al., 2005). To examine whether hedgehog signaling might be downstream of WNT11, we analyzed expression of the hedgehog signaling reporter *Patched-lacZ* (Goodrich et al., 1997) in *Wnt11* mutants. Our results demonstrated no alterations in *Patched*-driven beta-Galactosidase expression in *Wnt11* mutants (Fig. 5B), suggesting that WNT11 acts downstream of, or in parallel to hedgehog signaling in DMP formation.

Wnt2 mutants exhibit DMP defects, with reduced expression of the canonical WNT reporter AXIN2, and a reduction in Ki67+ proliferative cells within the DMP at E9.5 and E10.5 (Tian et al., 2010). Additionally, non-canonical WNT signaling via WNT5A represses canonical WNT signaling via a non-apoptotic CASPASE 3-mediated negative feedback loop (Abdul-Ghani et al., 2011; Bisson et al., 2015; Cohen et al., 2012). To investigate whether loss of WNT11 might result in alterations to canonical WNT signaling, and thus affect DMP proliferation, we examined *Axin2-lacZ* expression (Lustig et al., 2002). However, expression of *Axin2-lacZ* was not altered in germline *Wnt11* null embryos (Fig. 5C), suggesting that loss of WNT11 did not perturb canonical WNT signaling. Our previous studies demonstrated that canonical WNT signaling is upstream of WNT11 in OFT formation (Lin et al., 2007), leaving open the possibility of a similar regulatory pathway for WNT11 expression in DMP formation.

5. Conclusion

Altogether, our findings have demonstrated that WNT11 is required within myocardium for OFT formation. WNT11 was not required within myocardial, endocardial, epicardial, or neural crest lineages, but was required within *Isl1Cre* lineages, for DMP formation. DMP defects reflected a requirement for WNT11 in driving proliferation of the DMP itself. We further examined several signaling pathways important for inflow tract development and found that they remained unaltered. These results suggested that WNT11 works downstream of, or in parallel with, these pathways. It will be of future interest to more fully understand the interactions between WNT11 and other pathways required for DMP formation.

Supplementary Material

Refer to Web version on PubMed Central for supplementary material.

Acknowledgments

Confocal microscopy was performed at the UCSD Neuroscience Microscopy Core, which is supported by a NIH P30 core grant (NS047101). Imaging support by Jennifer Santini was greatly appreciated. We thank Drs. Anne-Monique Nuyt and Ying He (CHU Sainte Justine, Montreal) for the use of their Leica DMi8 microscope and assistance with imaging. We are grateful to the other members of the Evans lab for helpful discussions. This work was supported by NIH grants to S.M. Evans; a UC San Diego Cardiovascular Scholarship Award and a Postdoctoral Fellowship from the California Institute for Regenerative Medicine (CIRM) Interdisciplinary Stem Cell Training Program II to P.P. van Vliet; a Postdoctoral Fellowship (0525141Y) and Grant (SDG# 10SDG 2610105) from the American Heart Association to L. Lin; and grants from the Netherlands Organization for Scientific Research (NWO, 825.10.016) and the American Heart Association (13POST16480012) to C.J. Boogerd. J.F. Martin was supported by grants from the National Institutes of Health (DE 023177, HL 127717, HL 130804, and HL 118761 to

J.F. Martin) and the Vivian L. Smith Foundation (to J.F. Martin). J.F. Martin was supported by the Transatlantic Network of Excellence Award LeDucq Foundation Transatlantic Networks of Excellence in Cardiovascular Research14CVD01: “Defining the genomic topology of atrial fibrillation.”

References

Abdul-Ghani M, Dufort D, Stiles R, De Repentigny Y, Kothary R, Megeney LA. Wnt11 promotes cardiomyocyte development by caspase-mediated suppression of canonical Wnt signals. Mol Cell Biol. 2011; 31:163–178. http://dx.doi.org/10.1128/MCB.01539-09. [PubMed: 21041481]

Ai D, Fu X, Wang J, Lu MF, Chen L, Baldini A, Klein WH, Martin JF. Canonical Wnt signaling functions in second heart field to promote right ventricular growth. Proc Natl Acad Sci USA. 2007; 104:9319–9324. http://dx.doi.org/10.1073/pnas.0701212104. [PubMed: 17519332]

Ai D, Liu W, Ma L, Dong F, Lu MF, Wang D, Verzi MP, Cai C, Gage PJ, Evans S, Black BL, Brown NA, Martin JF. Pitx2 regulates cardiac left-right asymmetry by patterning second cardiac lineage-derived myocardium. Dev Biol. 2006; 296:437–449. http://dx.doi.org/10.1016/j.ydbio.2006.06.009. [PubMed: 16836994]

Anderson RH, Mori S, Spicer DE, Brown NA, Mohun TJ. Development and morphology of the ventricular outflow tracts. Pediatr Congenit Hear Surg Symp. 2016; 7:561–577. http://dx.doi.org/10.1177/2150135116651114.

Anderson RH, Spicer DE, Brown NA, Mohun TJ. The development of septation in the four-chambered heart. Anat Rec. 2014; 297:1414–1429. http://dx.doi.org/10.1002/ar.22949.

Bax NAM, Bleyl SB, Gallini R, Wisse LJ, Hunter J, Van Oorschot AAM, Mahtab EAF, Lie-Venema H, Goumans MJ, Betsholtz C, Gittenberger-de Groot AC. Cardiac malformations in Pdgfr α Mutant embryos are associated with increased expression of WT1 and Nkx2.5 in the second heart field. Dev Dyn. 2010; 239:2307–2317. http://dx.doi.org/10.1002/dvdy.22363. [PubMed: 20658695]

Bisson JA, Mills B, Helt JCP, Zwaka TP, Cohen ED. Wnt5a and Wnt11 inhibit the canonical Wnt pathway and promote cardiac progenitor development via the Caspase-dependent degradation of AKT. Dev Biol. 2015; 398:80–96. http://dx.doi.org/10.1016/j.ydbio.2014.11.015. [PubMed: 25482987]

Boogerd CJ, Aneas I, Sakabe N, Dirschinger RJ, Cheng QJ, Zhou B, Chen J, Nobrega MA, Evans SM. Probing chromatin landscape reveals roles of endocardial TBX20 in septation. J Clin Invest. 2016; 126:3023–3035. http://dx.doi.org/10.1172/JCI85350. [PubMed: 27348591]

Bosada, FM., Devasthali, V., Jones, KA., Stankunas, K. Wnt/β-catenin signaling enables developmental transitions during valvulogenesis; Development. 2016. p. 1041-1054.http://dx.doi.org/10.1242/dev.130575

Briggs LE, Burns TA, Lockhart MM, Phelps AL, Van den Hoff MJB, Wessels A. Wnt/β-catenin and sonic hedgehog pathways interact in the regulation of the development of the dorsal mesenchymal protrusion. Dev Dyn. 2016; 245:103–113. http://dx.doi.org/10.1002/dvdy.24339. [PubMed: 26297872]

Briggs, LE., Kakarla, J., Wessels, A. The pathogenesis of atrial and atrioventricular septal defects with special emphasis on the role of the dorsal mesenchymal protrusion. Differentiation. 2012. http://dx.doi.org/10.1016/j.diff.2012.05.006

Briggs LE, Phelps AL, Brown E, Kakarla J, Anderson RH, Van Den Hoff MJB, Wessels A. Expression of the bmp receptor alk3 in the second heart field is essential for development of the dorsal mesenchymal protrusion and atrioventricular septation. Circ Res. 2013; 112:1420–1432. http://dx.doi.org/10.1161/CIRCRESAHA.112.300821. [PubMed: 23584254]

Buckingham M, Meilhac S, Zaffran S. Building the mammalian heart from two sources of myocardial cells. Nat Rev Genet. 2005; 6:826–835. http://dx.doi.org/10.1038/nrg1710. [PubMed: 16304598]

Burns T, Yang Y, Hiriart E, Wessels A. The dorsal mesenchymal protrusion and the pathogenesis of atrioventricular septal defects. J Cardiovasc Dev Dis. 2016; 3:29. http://dx.doi.org/10.3390/jcdd3040029. [PubMed: 28133602]

Cai CL, Liang X, Shi Y, Chu PH, Pfaff SL, Chen J, Evans S. Isl1 identifies a cardiac progenitor population that proliferates prior to differentiation and contributes a majority of cells to the heart. Dev Cell. 2003; 5:877–889. http://dx.doi.org/10.1016/S1534-5807(03)00363-0. [PubMed: 14667410]

Cohen ED, Miller MF, Wang Z, Moon RT, Morrisey EE. Wnt5a and Wnt11 are essential for second heart field progenitor development. Development. 2012; 139:1931–1940. http://dx.doi.org/10.1242/dev.069377. [PubMed: 22569553]

Del Monte G, Casanova JC, Guadix JA, MacGrogan D, Burch JBE, Pérez-Pomares JM, De La Pompa JL. Differential notch signaling in the epicardium is required for cardiac inflow development and coronary vessel morphogenesis. Circ Res. 2011; 108:824–836. doi:http://dx.doi.org/10.1161/CIRCRESAHA.110.229062. [PubMed: 21311046]

Engleka KA, Manderfield LJ, Brust RD, Li L, Cohen A, Dymecki SM, Epstein JA. Islet1 derivatives in the heart are of both neural crest and second heart field origin. Circ Res. 2012; 110:922–926. http://dx.doi.org/10.1161/CIRCRESAHA.112.266510. [PubMed: 22394517]

Evans, SM., Yelon, D., Conlon, FL., Kirby, ML. Myocardial lineage development. Circ Res. 2010. http://dx.doi.org/10.1161/CIRCRESAHA.110.227405

Flaherty, MP., Dawn, B. Noncanonical Wnt11 signaling and cardiomyogenic differentiation. Trends Cardiovasc Med. 2008. http://dx.doi.org/10.1016/j.tcm.2008.12.001

Galli D, Dominguez JN, Zaffran S, Munk A, Brown NA, Buckingham ME. Atrial myocardium derives from the posterior region of the second heart field, which acquires left-right identity as Pitx2c is expressed. Development. 2008; 135:1157–1167. http://dx.doi.org/10.1242/dev.014563. [PubMed: 18272591]

Gillers BS, Chiplunkar A, Aly H, Valenta T, Basler K, Christoffels VM, Efimov IR, Boukens BJ, Rentschler S. Canonical Wnt signaling regulates atrioventricular junction programming and electrophysiological properties. Circ Res. 2015; 116:398–406. http://dx.doi.org/10.1161/CIRCRESAHA.116.304731. [PubMed: 25599332]

Goddeeris MM, Rho S, Petiet A, Davenport CL, Johnson GA, Meyers EN, Klingensmith J. Intracardiac septation requires hedgehog-dependent cellular contributions from outside the heart. Development. 2008; 135:1887–1895. http://dx.doi.org/10.1242/dev.016147. [PubMed: 18441277]

Goddeeris MM, Schwartz R, Klingensmith J, Meyers EN. Independent requirements for Hedgehog signaling by both the anterior heart field and neural crest cells for outflow tract development. Development. 2007; 134:1593–1604. (dev.02824)(pii). doi:/r10.1242/dev.02824. [PubMed: 17344228]

Goodrich LV, Milenković L, Higgins KM, Scott MP. Altered neural cell fates and medulloblastoma in mouse patched mutants. Science. 1997; 277:1109–1113. http://dx.doi.org/10.1126/science.277.5329.1109. [PubMed: 9262482]

Henderson DJ, Phillips HM, Chaudhry B. Vang-like 2 and noncanonical Wnt signaling in outfiow tract development. Trends Cardiovasc Med. 2006; 16:38–45. http://dx.doi.org/10.1016/j.tcm.2005.11.005. [PubMed: 16473760]

Hoffmann AD, Peterson MA, Friedland-Little JM, Anderson SA, Moskowitz IP. Sonic hedgehog is required in pulmonary endoderm for atrial septation. Development. 2009; 136:1761–1770. http://dx.doi.org/10.1242/dev.034157. [PubMed: 19369393]

Jiao K, Kulessa H, Tompkins K, Zhou Y, Batts L, Baldwin HS, Hogan BLM. An essential role of Bmp4 in the atrioventricular septation of the mouse heart. Genes Dev. 2003; 17:2362–2367. http://dx.doi.org/10.1101/gad.1124803. [PubMed: 12975322]

Kim JS, Virágh S, Moorman AF, Anderson RH, Lamers WH. Development of the myocardium of the atrioventricular canal and the vestibular spine in the human heart. Circ Res. 2001; 88:395–402. http://dx.doi.org/10.1161/01.RES.88.4.395. [PubMed: 11230106]

Kisanuki YY, Hammer RE, Miyazaki J, Williams SC, Richardson JA, Yanagisawa M. Tie2-Cre transgenic mice: a new model for endothelial cell-lineage analysis in vivo. Dev Biol. 2001; 230:230–242. http://dx.doi.org/10.1006/dbio.2000.0106. [PubMed: 11161575]

Kitamura K, Miura H, Miyagawa-Tomita S, Yanazawa M, Katoh-Fukui Y, Suzuki R, Ohuchi H, Suehiro A, Motegi Y, Nakahara Y, Kondo S, Yokoyama M. Mouse Pitx2 deficiency leads to anomalies of the ventral body wall, heart, extra- and periocular mesoderm and right pulmonary isomerism. Development. 1999; 126:5749–5758. http://dx.doi.org/10.1007/bf02401419. [PubMed: 10572050]

Lewis AE, Vasudevan HN, O' Neill AK, Soriano P, Bush JO. The widely used Wnt1-Cre transgene causes developmental phenotypes by ectopic activation of Wnt signaling. Dev Biol. 2013; 379:229–234. http://dx.doi.org/10.1016/j.ydbio.2013.04.026. [PubMed: 23648512]

Lin CJ, Lin CY, Chen CH, Zhou B, Chang CP. Partitioning the heart: mechanisms of cardiac septation and valve development. Development. 2012; 139:3277–3299. http://dx.doi.org/10.1242/dev.063495. [PubMed: 22912411]

Lin L, Bu L, Cai CL, Zhang X, Evans S. Isl1 is upstream of sonic hedgehog in a pathway required for cardiac morphogenesis. Dev Biol. 2006; 295:756–763. http://dx.doi.org/10.1016/j.ydbio.2006.03.053. [PubMed: 16687132]

Lin L, Cui L, Zhou W, Dufort D, Zhang X, Cai CL, Bu L, Yang L, Martin J, Kemler R, Rosenfeld MG, Chen J, Evans SM. Beta-catenin directly regulates Islet1 expression in cardiovascular progenitors and is required for multiple aspects of cardiogenesis. Proc Natl Acad Sci USA. 2007; 104:9313–9318. http://dx.doi.org/10.1073/pnas.0700923104. [PubMed: 17519333]

Lustig B, Jerchow B, Sachs M, Weiler S, Pietsch T, Karsten U, van de Wetering M, Clevers H, Schlag PM, Birchmeier W, Behrens J. Negative feedback loop of Wnt signaling through upregulation of conductin/axin2 in colorectal and liver tumors. Mol Cell Biol. 2002; 22:1184–1193. http://dx.doi.org/10.1128/MCB.22.4.1184. [PubMed: 11809809]

Ma Q, Zhou B, Pu WT. Reassessment of Isl1 and Nkx2-5 cardiac fate maps using a Gata4-based reporter of Cre activity. Dev Biol. 2008; 323:98–104. http://dx.doi.org/10.1016/j.ydbio.2008.08.013. [PubMed: 18775691]

Madisen L, Zwingman TA, Sunkin SM, Oh SW, Zariwala HA, Gu H, Ng LL, Palmiter RD, Hawrylycz MJ, Jones AR, Lein ES, Zeng H. A robust and high-throughput Cre reporting and characterization system for the whole mouse brain. Nat Neurosci. 2010; 13:133–140. http://dx.doi.org/10.1038/nn.2467. [PubMed: 20023653]

Majumdar A, Vainio S, Kispert A, McMahon J, McMahon AP. Wnt11 and Ret/Gdnf pathways cooperate in regulating ureteric branching during metanephric kidney development. Development. 2003; 130:3175–3185. http://dx.doi.org/10.1242/dev.00520. [PubMed: 12783789]

Mercer EH, Hoyle GW, Kapur RP, Brinster RL, Palmiter RD. The dopamine beta-hydroxylase gene promoter directs expression of E. coli lacZ to sympathetic and other neurons in adult transgenic mice. Neuron. 1991; 7:703–716. 0896-6273(91)90274-4(pii). [PubMed: 1742021]

Mommersteeg MTM, Brown NA, Prall OWJ, De Gier-De Vries C, Harvey RP, Moorman AFM, Christofiels VM. Pitx2c and Nkx2-5 are required for the formation and identity of the pulmonary myocardium. Circ Res. 2007; 101:902–909. http://dx.doi.org/10.1161/CIRCRESAHA.107.161182. [PubMed: 17823370]

Mommersteeg MTM, Soufan AT, De Lange FJ, Van Den Hoff MJB, Anderson RH, Christofiels VM, Moorman AFM. Two distinct pools of mesenchyme contribute to the development of the atrial septum. Circ Res. 2006; 99:351–353. http://dx.doi.org/10.1161/01.RES.0000238360.33284.a0. [PubMed: 16873717]

Nagy II, Railo A, Rapila R, Hast T, Sormunen R, Tavi P, Räsänen J, Vainio SJ. Wnt-11 signalling controls ventricular myocardium development by patterning N-cadherin and β-catenin expression. Cardiovasc Res. 2010; 85:100–109. http://dx.doi.org/10.1093/cvr/cvp254. [PubMed: 19622544]

Parker SE, Mai CT, Canfield MA, Rickard R, Wang Y, Meyer RE, Anderson P, Mason CA, Collins JS, Kirby RS, Correa A. Updated national birth prevalence estimates for selected birth defects in the United States, 2004–2006. Birth Defects Res Part A - Clin Mol Teratol. 2010; 88:1008–1016. http://dx.doi.org/10.1002/bdra.20735. [PubMed: 20878909]

Prall OWJ, Menon MK, Solloway MJ, Watanabe Y, Zaffran S, Bajolle F, Biben C, McBride JJ, Robertson BR, Chaulet H, Stennard FA, Wise N, Schaft D, Wolstein O, Furtado MB, Shiratori H, Chien KR, Hamada H, Black BL, Saga Y, Robertson EJ, Buckingham ME, Harvey RP. An Nkx2-5/Bmp2/Smad1 negative feedback loop controls heart progenitor specification and proliferation. Cell. 2007; 128:947–959. http://dx.doi.org/10.1016/j.cell.2007.01.042. [PubMed: 17350578]

Qyang Y, Martin-Puig S, Chiravuri M, Chen S, Xu H, Bu L, Jiang X, Lin L, Granger A, Moretti A, Caron L, Wu X, Clarke J, Taketo MM, Laugwitz KL, Moon RT, Gruber P, Evans SM, Ding S, Chien KR. The renewal and differentiation of Isl1+ cardiovascular progenitors are controlled by a

Wnt/β-Catenin pathway. Cell Stem Cell. 2007; 1:165–179. http://dx.doi.org/10.1016/j.stem.2007.05.018. [PubMed: 18371348]

Sinha T, Lin L, Li D, Davis J, Evans S, Wynshaw-Boris A, Wang J. Mapping the dynamic expression of Wnt11 and the lineage contribution of Wnt11-expressing cells during early mouse development. Dev Biol. 2015; 398:177–192. http://dx.doi.org/10.1016/j.ydbio.2014.11.005. [PubMed: 25448697]

Snarr BS, O' Neal JL, Chintalapudi MR, Wirrig EE, Phelps AL, Kubalak SW, Wessels A. Isl1 expression at the venous pole identifies a novel role for the second heart field in cardiac development. Circ Res. 2007a; 101:971–974. http://dx.doi.org/10.1161/CIRCRESAHA.107.162206. [PubMed: 17947796]

Snarr BS, Wirrig EE, Phelps AL, Trusk TC, Wessels A. A spatiotemporal evaluation of the contribution of the dorsal mesenchymal protrusion to cardiac development. Dev Dyn. 2007b; 236:1287–1294. http://dx.doi.org/10.1002/dvdy.21074. [PubMed: 17265457]

Tian Y, Yuan L, Goss AM, Wang T, Yang J, Lepore JJ, Zhou D, Schwartz RJ, Patel V, Cohen ED, Morrisey EE. Characterization and in vivo pharmacological rescue of a Wnt2-Gata6 pathway required for cardiac inflow tract development. Dev Cell. 2010; 18:275–287. http://dx.doi.org/10.1016/j.devcel.2010.01.008. [PubMed: 20159597]

Uysal-Onganer, P., Kypta, RM. Wnt11 in 2011 - the regulation and function of a non-canonical Wnt. Acta Physiol. 2012. http://dx.doi.org/10.1111/j.1748-1716.2011.02297.x

Washington Smoak I, Byrd NA, Abu-Issa R, Goddeeris MM, Anderson R, Morris J, Yamamura K, Klingensmith J, Meyers EN. Sonic hedgehog is required for cardiac outflow tract and neural crest cell development. Dev Biol. 2005; 283:357–372. S0012-1606(05)(00264-2 (pii)/r. DOI: 10.1016/j.ydbio.2005.04.029 [PubMed: 15936751]

Wessels A, van den Hoff MJB, Adamo RF, Phelps AL, Lockhart MM, Sauls K, Briggs LE, Norris RA, van Wijk B, Perez-Pomares JM, Dettman RW, Burch JBE. Epicardially derived fibroblasts preferentially contribute to the parietal leaflets of the atrioventricular valves in the murine heart. Dev Biol. 2012; 366:111–124. http://dx.doi.org/10.1016/j.ydbio.2012.04.020. [PubMed: 22546693]

Yang L, Cai CL, Lin L, Qyang Y, Chung C, Monteiro RM, Mummery CL, Fishman GI, Cogen A, Evans S. Isl1Cre reveals a common Bmp pathway in heart and limb development. Development. 2006; 133:1575–1585. http://dx.doi.org/10.1242/dev.02322. [PubMed: 16556916]

Zhou W, Lin L, Majumdar A, Li X, Zhang X, Liu W, Etheridge L, Shi Y, Martin J, Van de Ven W, Kaartinen V, Wynshaw-Boris A, McMahon AP, Rosenfeld MG, Evans SM. Modulation of morphogenesis by noncanonical Wnt signaling requires ATF/CREB family-mediated transcriptional activation of TGFbeta2Nat. Genet. 2007; 39:1225–1234. http://dx.doi.org/10.1038/ng2112.

Appendix A. Supporting information

Supplementary data associated with this article can be found in the online version at doi: 10.1016/j.ydbio.2017.06.021.

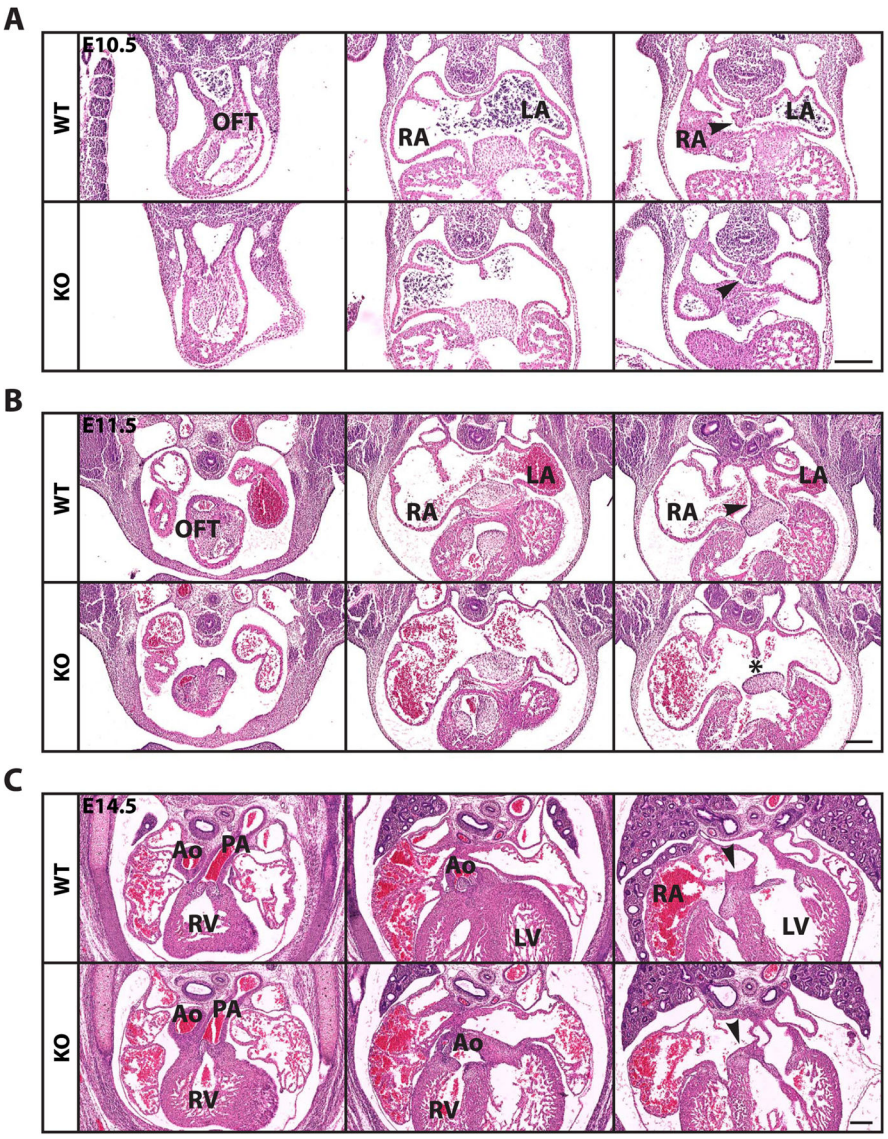

Fig. 1. Histological analysis of cardiac defects in germline Wnt11 null embryos

Hematoxylin & eosin stainings of wild-type (WT) and germline *Wnt11* knock-out (KO) embryos at E10.5 (A), E11.5 (B), and E14.5 (C). Left panels: anterior sections showing outflow tract (OFT). Middle panels: medial sections showing AV region. Right panels: posterior sections showing DMP region. E10.5 and E11.5 WT embryos show normal growth and rotation of the OFT (A–B, left panels), leading to proper alignment of the aorta with the left ventricle and pulmonary artery with the right ventricle at E14.5 (C, left panel). In contrast, *Wnt11* KO embryos showed defective growth and malrotation of the OFT at E10.5 (A) and E11.5 (B), leading to OFT defects such as double outlet right ventricle (DORV), where both the aorta and pulmonary artery connect to the right ventricle, at E14.5 (C). We did not observe any differences in the primary atrial septum or AV cushion morphology between WT and KO at any of these stages (A–C, middle panels), indicating that these parts of the AV septal complex were not defective. Posterior sections showed that, in E10.5 WT

embryos, the right-sided DMP protrudes normally into the atrial lumen. In contrast, KO embryos lack this protruding structure (A, right panels, arrowhead). At E11.5 (B), the DMP (arrowhead) has closed the opening between the primary atrial septum dorsally and the AV cushions ventrally in WT embryos (B, right panels). In E11.5 KO embryos, the DMP fails to close this opening (asterisk). At E14.5 (C), the DMP-derived myocardium has formed a solid connection between the atrial septum and AV cushions in WT embryos (C, right panels, arrowhead). In E14.5 KO embryos, reduced DMP growth has led to a smaller DMP-derived myocardial structure. Scale bars are 200 μm.

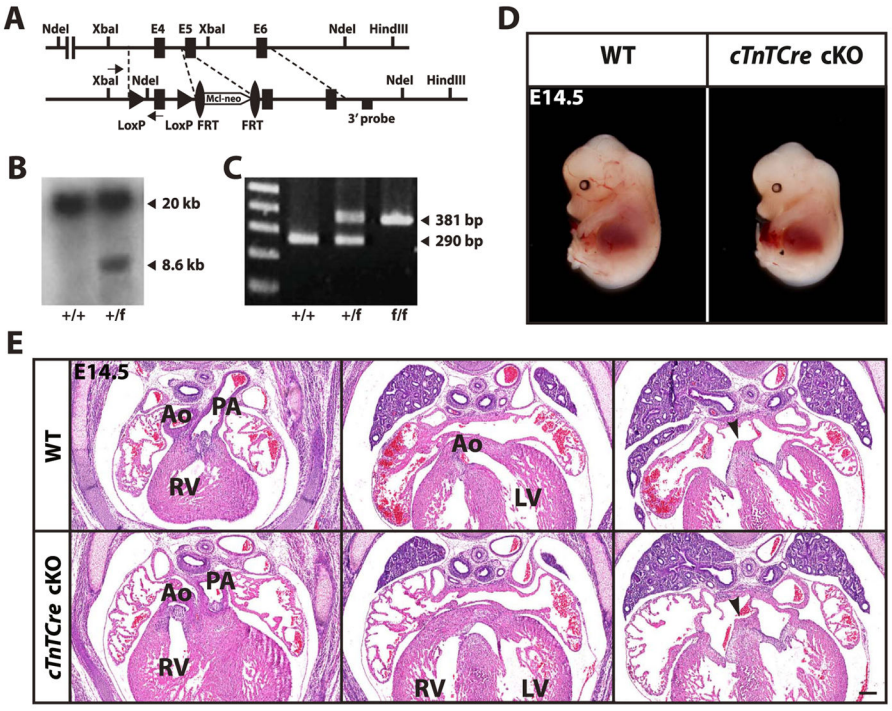

Fig. 2. Conditional deletion of Wnt11 with cTnTCre

A–C) Generation of the *Wnt11 flox/flox* line. (A) Schematic diagram of the wild-type allele (top) and targeting construct (bottom). Black boxes indicate exons. Black triangles indicate loxP insertions. Arrows indicate location of primers for genotyping. Black oval circles indicate FRT sites. (B) Southern blot for the 3′ probe (indicated in A) on digested genomic DNA to confirm insertion of the target sequence. +/+ wild-type control. +/f: hemizygous *Wnt11 flox/+* line. (C) Agarose gel showing PCR products after genotyping on genomic DNA from tail biopsies with primers indicated in A. Wild-type allele: 290 bp. Mutated allele: 381 bp. +/+ wild-type control. +/f: hemizygous *Wnt11 flox/+* line. f/f: homozygous *Wnt11 flox/flox* line. (D–E) Whole mount (D) and histological analysis (E) after *cTnTCre-lox* deletion of *Wnt11*. Compared to wild-type (WT) controls, E14.5 *cTnTCre; Wnt11* null/flox conditional knockout embryos (*cTnTCre* cKO) show normal overall morphology. (E) Whereas E14.5 WT controls show normal OFT, AV, and DMP development (top panels), E14.5 *cTnTCre; Wnt11* null/flox embryos show connections between aorta and right ventricle, and between pulmonary artery and left ventricle, indicating transposition of the great arteries (TGA, bottom panels). The DMP-derived myocardium in E14.5 cKO embryos is similar to that in WT embryos (arrowheads). Scale bars are 200 μm.

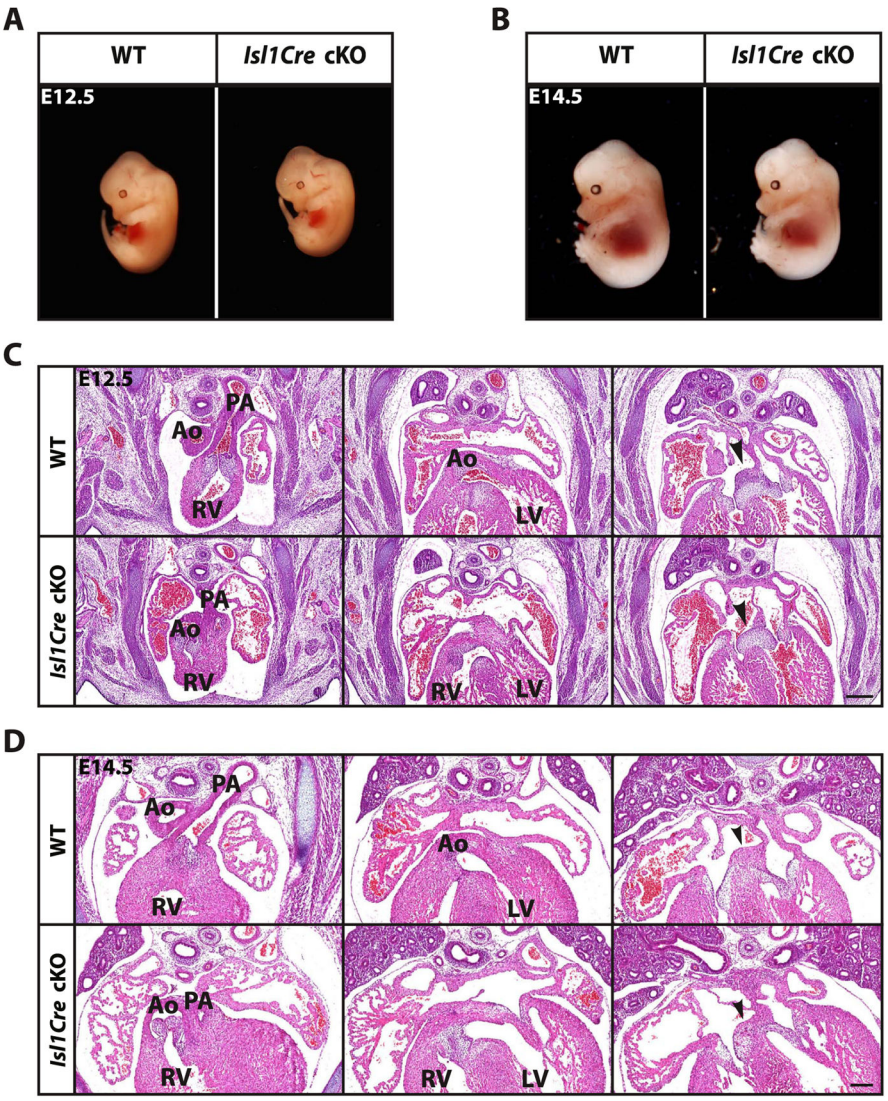

Fig. 3. Conditional deletion of Wnt11 with Isl1Cre

(A–B) Whole mount analysis of E12.5 and E14.5 embryos showed that *Isl1Cre; Wnt11* null/flox conditional knockout embryos (*Isl1Cre* cKO) were morphologically normal. Histological analysis at E12.5 (C) and E14.5 (D) revealed that *Isl1Cre; Wnt11* cKO embryos develop outflow tract defects at E12.5 (DORV, C, left panel) and E14.5 (TGA, D, left panel) and reduced DMP growth at E12.5 and E14.5 (arrowheads, C, D, right panels). The atrial septum and AV cushions were morphologically normal (C, D, middle panels). Scale bars are 200 μm.

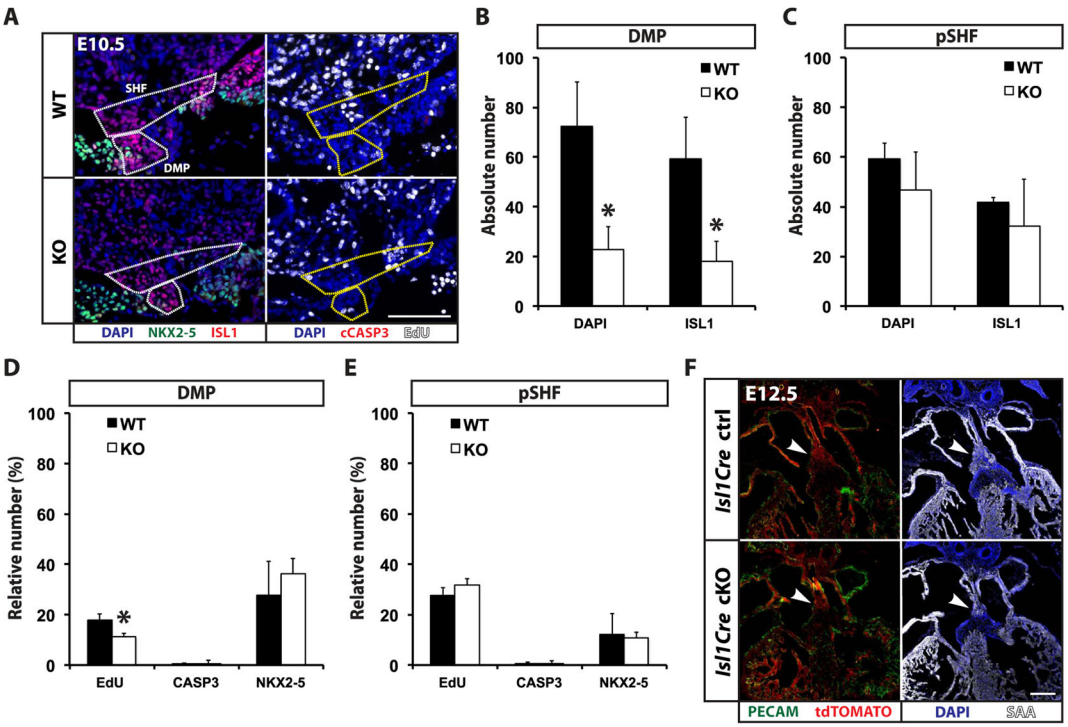

Fig. 4. Reduced proliferation is correlated to DMP hypoplasia

(A, left panels) Immunostaining for NKX2-5 (green) and ISL1 (red) in E10.5 WT and *Wnt11* KO embryos. Nuclei are stained with DAPI (blue). SHF and DMP are indicated with dashed lines. WT embryos showed an ISL1+ DMP that protrudes from the SHF into the atrial lumen between the dorsal walls of the NKX2.5+ atrial myocardium. KO embryos showed a much reduced and less protruding DMP. Scale bar is 100 μm. (B–C) Quantification of total nuclei (DAPI) and ISL1+ cells confirmed that there were significantly less DAPI+ nuclei and ISL1+ cells in the KO DMP when compared to WT (B, asterisks: $p < 0.05$). No differences were observed in the pSHF of KO versus WT embryos (C). (A, right panels) Immunostaining for cleaved CASPASE 3 (cCasp3, red) and EdU (white) in consecutive sections showed proliferative cells in both SHF and DMP, but little to no apoptosis. Scale bar is 100 μm. (D–E) Quantification of A showed significantly less proliferation in the reduced DMP of KO embryos when compared to WT (D, asterisks: $p < 0.05$). In contrast, no differences were observed in the pSHF (E). (F) Immunostaining for PECAM/CD31 (green) and sarcomeric actin (SAA, white) in E12.5 Isl1Cre control and *Isl1Cre; Wnt11* conditional knock-out embryos (Isl1Cre cKO). Nuclei are stained with DAPI (blue) and the *Isl1Cre; tdTomato* lineage is shown in red. Although the *Isl1Cre*-derived DMP (arrowhead, left panels) in *Isl1Cre; Wnt11* cKO embryos was smaller compared to controls, there was no difference in myocardial differentiation (right panels). Scale bar is 200 μm.

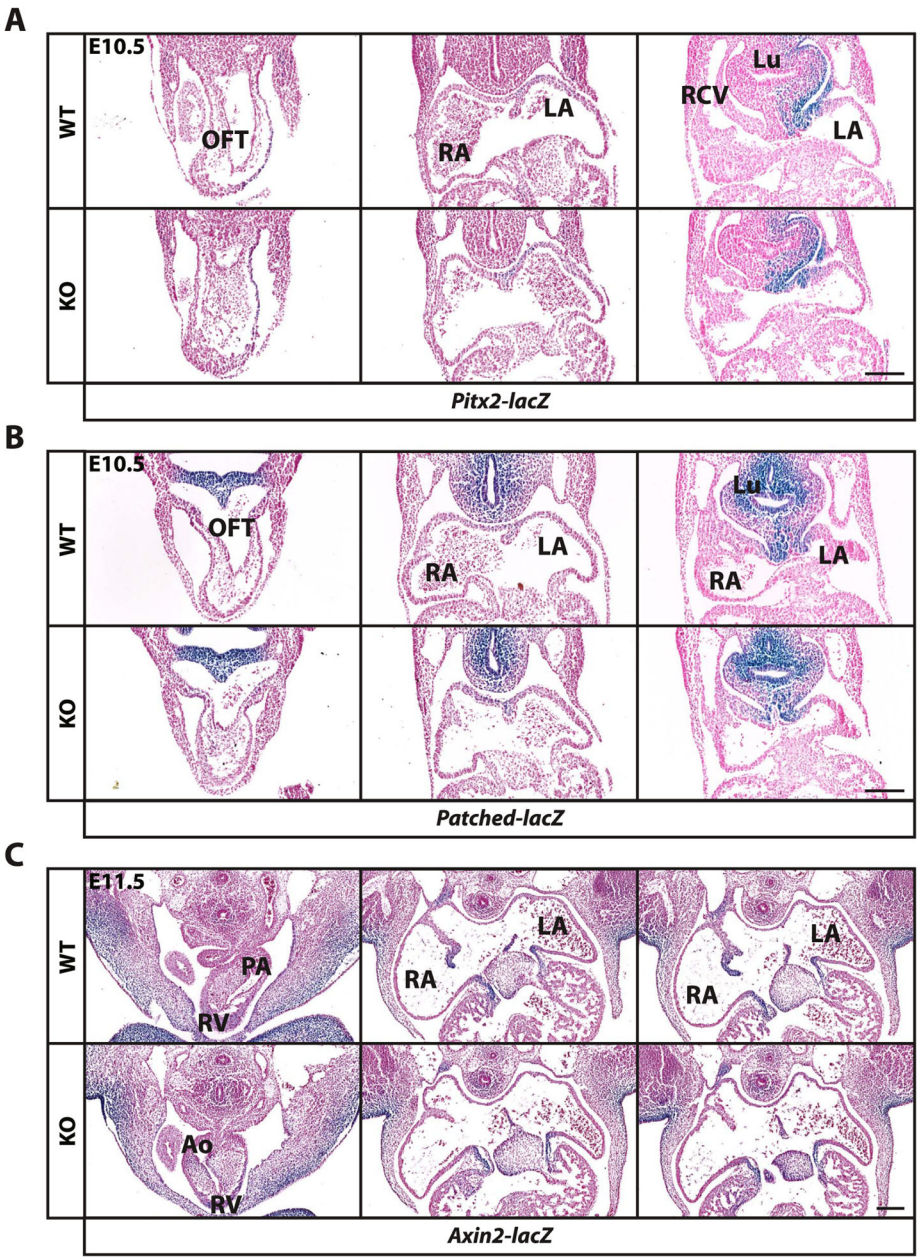

Fig. 5. Germline Wnt11 null defects are not associated with altered Pitx2-, Patched-, or Axin2-lacZ reporter expression

X-gal staining of Wnt11 WT and KO embryos heterozygous for Pitx2-lacZ (A), Patched-lacZ (B), or Axin2-lacZ (C). Nuclei were counterstained with Nuclear Fast Red. Although KO embryos showed OFT and DMP defects similar to those found during histological analysis (Fig. 1), no differences were observed in lacZ reporter expression in the OFT, pharyngeal mesoderm (left panels), AV region (middle panels), pSHF, DMP, or foregut endoderm (right panels). Scale bars are 200 μm.